DEUTSCHES ELEKTRONEN-SYNCHROTRON DESY

HIGH ENERGY TRENDS IN e^+e^- PHYSICS

(Rapporteur talk given at the 1979 EPS International Conference
on High Energy Physics, Geneva, 27 June - 4 July 1979)

by

Günter Wolf

*Deutsches Elektronen-Synchrotron DESY, Hamburg, Germany*

NOTKESTRASSE 85 · 2 HAMBURG 52

To be sure that your preprints are promptly included in the
HIGH ENERGY PHYSICS INDEX ,
send them to the following address (if possible by air mail) :

HIGH ENERGY TRENDS IN e^+e^- PHYSICS[*]

Günter Wolf

Deutsches Elektronen-Synchrotron DESY, Hamburg, Germany

1. INTRODUCTION

With the advent of PETRA the Q^2 range over which e^+e^- annihilations can be studied has been extended by an order of magnitude:

	SPEAR/DORIS I	DORIS II	PETRA
Q^2_{max}	~60 GeV²	100 GeV²	1000 GeV²

Although still preliminary and limited in statistics the data convey already a clear and exciting picture of what is happening at these high energies in certain areas.

As it turns out many things become simpler at high energies. For instance the occurence of jets is no longer the result of a complex analysis but can be seen with the naked eye. Fig. 1 shows a jet event as seen by MARK J. The hadronic showers are contained in two narrow cones.

Another example is the production of the heavy lepton τ. It took around 2 years of data taking at energies between 4 and 5 GeV in order to establish the existence of the τ. At PEP and PETRA energies the existence of the τ would have been firmly demonstrated within a month of running. This may be seen from Fig. 2 which displays a typical τ event of the kind

$$e^+e^- \to \tau^- \qquad \tau^+$$
$$\quad \lfloor_{\to \nu} + \text{3 charged} \qquad \lfloor_{\to \mu^+ \nu \bar{\nu}}$$

observed at 13 GeV. The probability for hadronic events of this topology with which τ events could be confused is very small.

Other features of e^+e^- analyses become more difficult at high energies and require care. One of them is the separation of annihilation from two photon events. While at low energies two photon contributions are mostly of the order of a few percent at PETRA energies the relative proportion of the two processes is reversed. However, e.g. by summing the total visible hadron energy a separation of the two processes can be achieved to an accuracy of a few percent. This is illustrated in Fig. 3 showing the sum of the observed charged and neutral energy as measured by PLUTO at 27.4 GeV.

2. STATUS OF PETRA

The new DESY e^+e^- colliding ring PETRA (= Positron Electron Tandem Ring Anlage) was

---
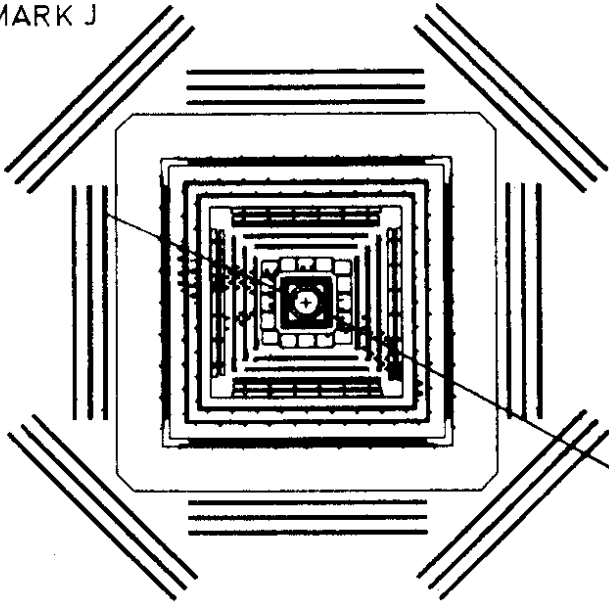
MARK J

Fig.1 Hadron event observed in the MARK J detector at 27.4 GeV.

TASSO
27.4GeV
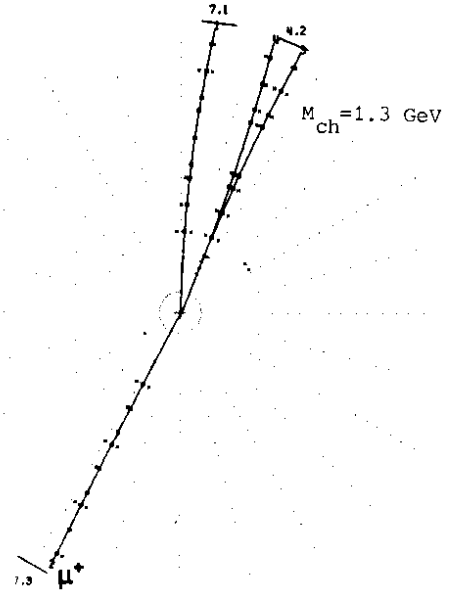
$M_{ch}=1.3$ GeV

μ^+

Fig.2 Candidate for τ pair production,
$e^+e^- \to \tau^+ \quad \tau^-$
$ \mid_{\to\mu^+\nu\nu} \mid_{\to\nu+} \text{3charged}$
by TASSO at 13 GeV.

$e^+ e^- \longrightarrow X + \cdots$
$\underbrace{}_{\text{visible}}$

N

PLUTO
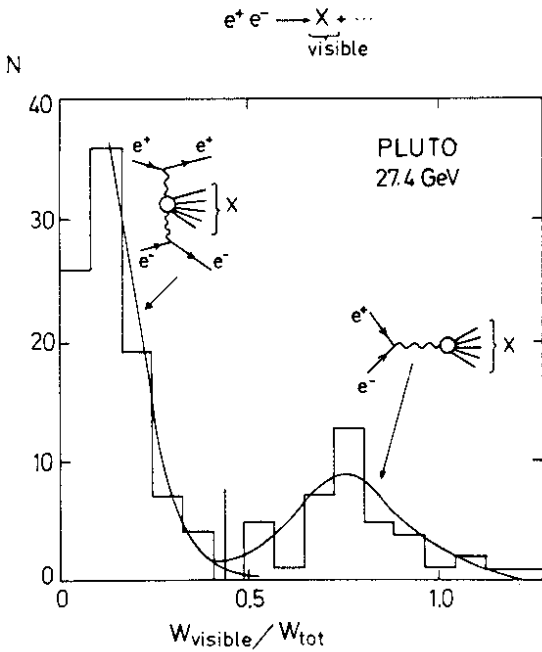27.4 GeV

$W_{visible}/W_{tot}$

Fig.3 Distribution of the total visible energy as observed by PLUTO at 27.4 GeV. The curves indicate the shape of the contributions expected from two photon exchange and one photon annihilation.
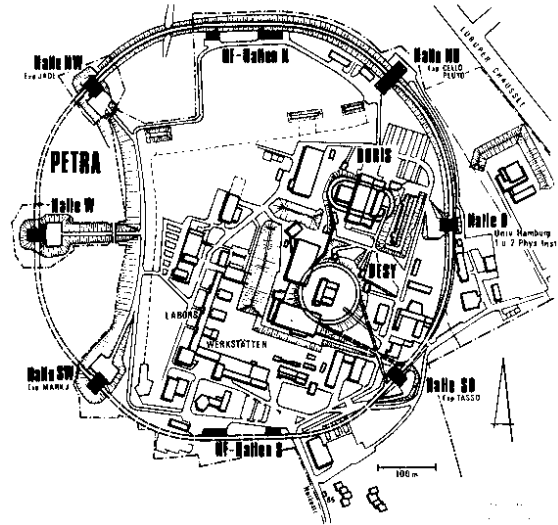
Fig.4 Layout of PETRA

gradually brought into operation in the second half of last year. Fig. 4 shows a layout of
the accelerator complex with the synchrotron (DESY) serving as injector and the storage
ring DORIS as accumulator for positrons. Some of the PETRA parameters are listed in Table I.
There are four short and four long straight sections. Two of the long straight sections are
used for the accelerating RF structures. The other six straight sections are available for
experiments.

At present five experiments have been installed or are being setup in the four short
sections:

North-East:	PLUTO, CELLO
North-West:	JADE
South-West:	MARK J
South-East:	TASSO

The number of RF cavities and therefore the maximum energy attainable has been/is being
increased in steps. Until February of this year four RF cavities were used providing a
maximum total energy of $W = 2E_{beam}$ = 22 GeV. With this configuration MARK J, PLUTO and
TASSO have   taken data at W = 13 and 17 GeV. Since March 32 cavities are installed
increasing the maximum energy to 32 GeV. The three experiments mentioned above, together
with JADE which has moved into the ring just recently, have carried out measurements at
27.4 GeV. By the end of this year a total of 64 cavities will be available allowing PETRA
to reach energies as high as W = 38 GeV.

The maximum luminosity obtained at 27.4 GeV was $3 \cdot 10^{30}$ $cm^{-2}sec^{-1}$ with two positron
and two electron bunches and 8 mA current per beam.

<div align="center">

Table I

PETRA parameters

</div>

maximum beam energy	19 GeV
circumference	2.3 km
magnetic bending radius	192 m
number of interaction regions	6
length of interaction region	15 m
RF frequency	500 MHz
number of klystrons	8
power per klystron	0.5 MW
max. number of cavities	64

3. ENERGY DEPENDENCE OF R

The total cross section σ_{tot} for

$$e^+e^- \rightarrow hadrons$$

is given in terms of the cross section for μ pair production ($\sigma(e^+e^- \rightarrow \mu^+\mu^-) \simeq \frac{4\pi\alpha^2}{3\,s} =$
$\frac{87.7 \text{ nb}}{s \text{ (GeV}^2)}$. $s = W^2$ = square of total c.m. energy):

$$R = \sigma_{tot} / \sigma_{\mu\mu}$$

Fig. 5 shows a compilation of measurements from near threshold up to an energy of W = 3 GeV.[1-5]
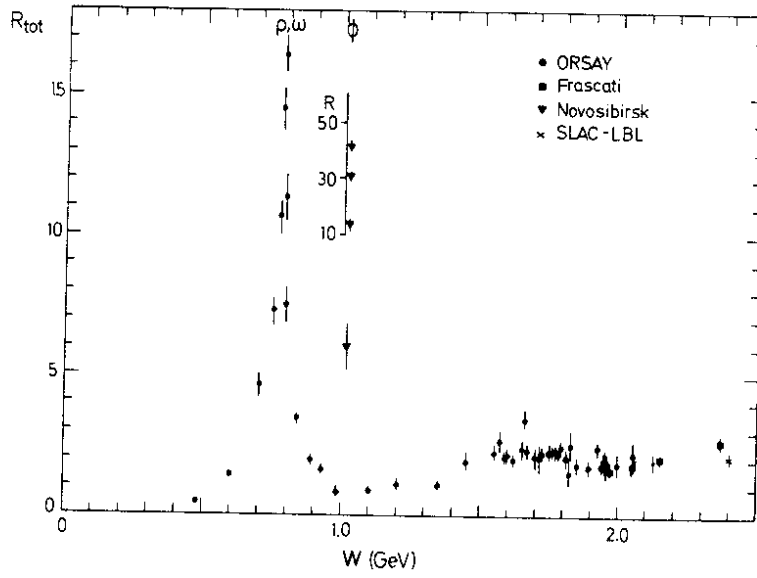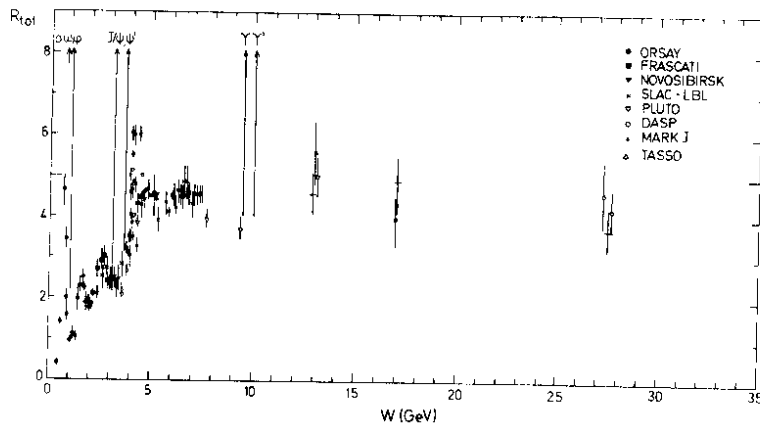
Fig.5 Measurements of R from Refs. 1-4.

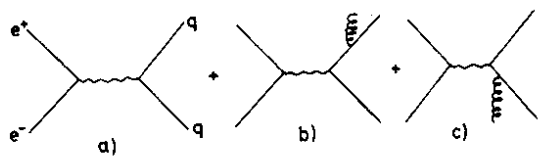Fig.6 Measurements of R from Refs. 1 - 4, 6 - 10.

Fig.7 Diagram for quark pair production (a) plus gluon corrections (b), (c)
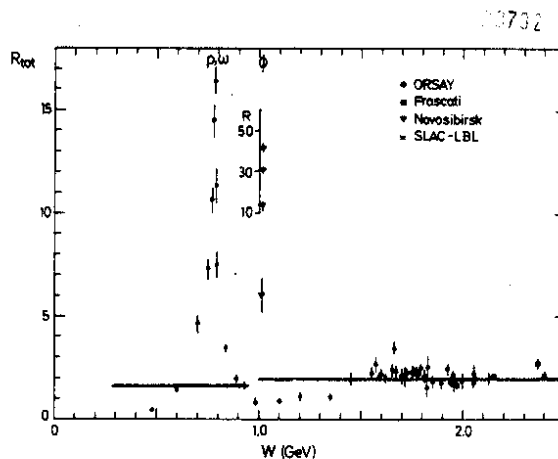

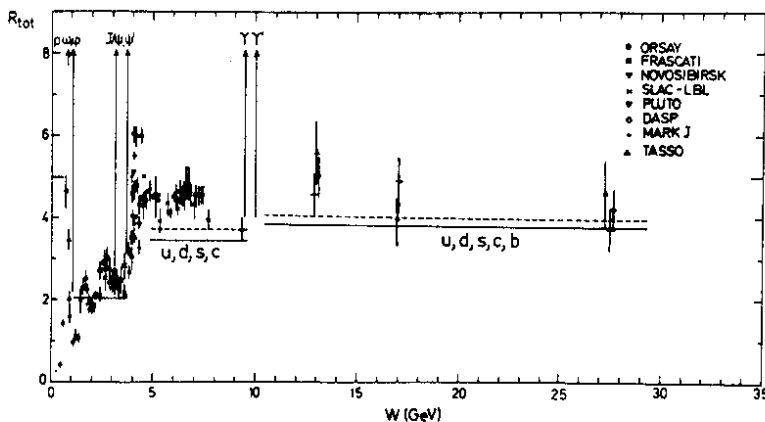Fig.8 Measurements of R and the prediction of the quark model (solid lines)

Fig.9 Measurements of R. The solid lines show the prediction from the quark model. The dashed lines show the quark model predictions corrected for gluon emission.

The error bars shown in this and the subsequent figure are only statistical. The systematic uncertainties are at the level of 10 - 20 %. The new data from ADONE[2] and DCI[3] presented at the Tokyo conference have clarified the behaviour of R in the region between 1 and 2 GeV. Below 1 GeV is the regime of the ground state vector mesons ρ, ω and ϕ. Above 1 GeV R shows a rather smooth behaviour despite the fact that individual channels (e.g. 4π, 5π) are dominated by the excitation of higher mass vector mesons such as the $\rho(1500)$, the $\omega(1700)$ and possibly others[2,3]. We see that R is near 1 between 1.1 and 1.4 GeV and then rising to a level of about 2 above 1.5 GeV. The rise is probably related to the onset of K production; above 1.6 GeV final states with kaons contribute approximately one unit in R[5].

The high energy region[4,6-10] together with the low energy data is shown in Fig. 6. The highest energy data points at 13, 17 and 27.4 GeV were measured by the MARK J[8], PLUTO[9] and TASSO[10] experiments at PETRA. A description of these new setups and the analysis procedures can be found in the reports of Drs. Branson[8], Blobel[9] and Cashmore[10] to this conference. The R values measured in these experiments are listed in Table 2:

Table 2

Measured R values at high energies

	13 GeV	17 GeV	27.4 GeV
MARK J	$4.6 \pm 0.5 \pm 0.7$	$4.9 \pm 0.5 \pm 0.7$	$3.7 \pm 0.5 \pm 0.7$
PLUTO	$5.0 \pm 0.5 \pm 1.0$	$4.3 \pm 0.5 \pm 0.8$	$4.2 \pm 0.5 \pm 0.8$
TASSO	$5.6 \pm 0.7 \pm 1.1$	$4.0 \pm 0.7 \pm 0.8$	$4.6 \pm 0.8 \pm 0.9$

The errors give the statistical and the systematic uncertainties.
The outstanding features of R as observed above 3 GeV are the spikes from the excitation of $J/\psi, \psi', \ldots$ and of Υ, Υ' ,... plus the fact that in between the two particle families and above Υ, Υ' R is almost constant.

Note that the final value for R measured by PLUTO just below the Υ at 9.4 GeV is $3.7 \pm 0.3 \pm 0.5$. The high energy data points are consistent with R being constant or slightly falling between 13 and 27.4 GeV. A rise of R e.g. by two units from 17 to 27.4 GeV appears to be improbable.

The simple quark model is in striking agreement with the general behaviour of R. In the quark model hadron production proceeds via the formation of a quark antiquark pair (see Fig. 7). Assuming that the produced quarks turn into hadrons with unit probability R measures the sum of the square of the quark charges:

$$R(s) = \sum \frac{\sigma_{q\bar{q}}}{\sigma_{\mu\mu}} = 3 \sum e_q^2 \qquad (1)$$

$$q = u,d,s,c,\ldots$$

$$M_q > W/2$$

The factor of 3 accounts for the colour degree of freedom. R is predicted to be a step function with a rise above each new quark threshold. The comparison with the data is shown in Figs. 8 and 9. Up to 3 GeV only u,d and s contribute and therefore R = 2 in good accord with the data between 1.5 and 3 GeV. Above charm threshold (near 4 GeV) R should rise to a level of 3.3. The data are larger mainly because of resonance effetcs; above 4.5 GeV the measured R values seem to descend slowly towards the quark model value. Beyond the Υ, Υ'...

family the data are again higher than the theoretical value of 3.7 but tend to approch this value as the energy increases. A possible sixth quark contribution will be discussed later.

In QCD gluon emission (diagrams b and c in Fig. 7) modifies the result of the quark model; R_o:

$$R = R_o \left(1 + \frac{\alpha_s(s)}{\pi}\right) \tag{2}$$

Here, α_s measures the strength of the gluon quark coupling

$$\alpha_s = \frac{12\pi}{(33-2\ N_f)\ \ln\ s/\Lambda^2}$$

with N_f being the number of quark flavours (e.g. N_f = 4 for u,d,s,c) and Λ a constant which from neutrino experiments is found to be ~500 MeV. The QCD correction increases the predicted R values by approximately 10 % (see dashed lines in Fig. 9). This is well within the accuracy of the experimental data points.

4. GROSS FEATURES OF THE FINAL STATES

a) Multiplicity

In Fig. 10 the average charge multiplicity $<n_{ch}>$ is plotted as a function of s[2,9-11]. Although the data are preliminary since most of them have not yet been published and corrections for acceptance, for photons converting in the beampipe, etc. may not always have been made in the same way, they suggest, that the multiplicity above ~10 GeV is rising (logarithmically) faster than at lower energies.

The dashed curve in Fig. 10 gives the energy dependence of $<n_{ch}>$ for pp collisions[12]. The pp multiplicity is lower by 0.5 to 1 units but has almost the same behaviour with energy.

A good fit to the e^+e^- data is obtained with the function (see solid curve)

$$<n_{ch}> = 2 + 0.2\ \ln s + 0.18\ (\ln s)^2$$

The decomposition of $<n_{ch}>$ into charged pion, kaons and nucleons is shown in Fig. 11 for the 3.6 to 5.2 GeV region[11]: the majority of the charged hadrons are pions (~83 %); kaons account for ~15 %, protons and antiprotons for ~2 %. As the energy increases and the phase space effect due to the larger kaon mass is reduced one expects the fraction of kaons to rise. Whether this is so remains to be seen.

b) Inclusive particle spectra

The differential cross section for producing a particle h with momentum and energy P,E and angle Θ relative to the beam axis (see Fig. 12) can be expressed in terms of two structure functions $\overline{W}_1$ and $\overline{W}_2$ which are closely related to W_1 and W_2 measured in inelastic lepton hadron scattering:

$$\frac{d^2\sigma}{dx d\Omega} = \frac{\alpha^2}{s}\ \beta x\ \{m\overline{W}_1 + \frac{1}{4}\ \beta^2\ x\ \nu\overline{W}_2\ \sin^2\Theta\} \tag{4}$$

where m is the mass of h, β = P/E, x = E/E_{beam} = $2E/\sqrt{s}$ and ν is the energy of the virtual photon as seen in the h rest system, ν = $E/m\ \sqrt{s}$.
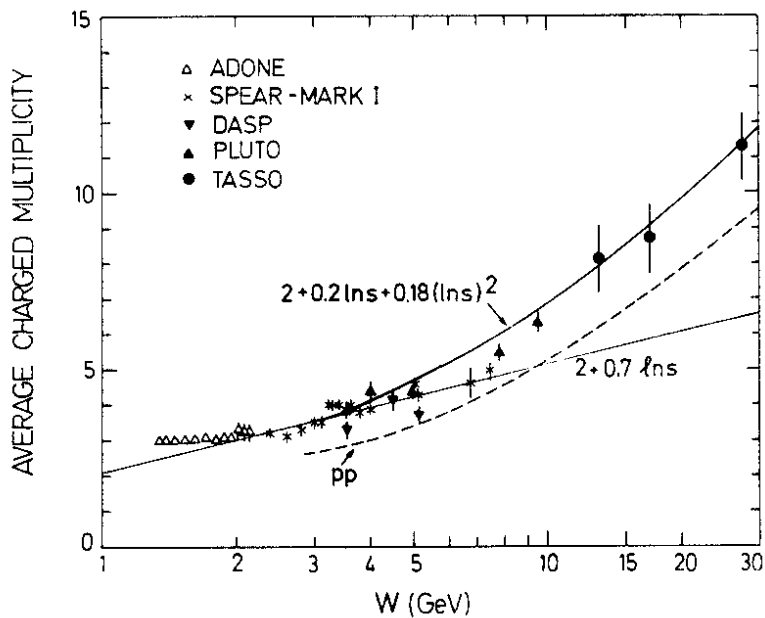
Fig.10 Average charge multiplicity (Refs. 2, 9-11). The dashed
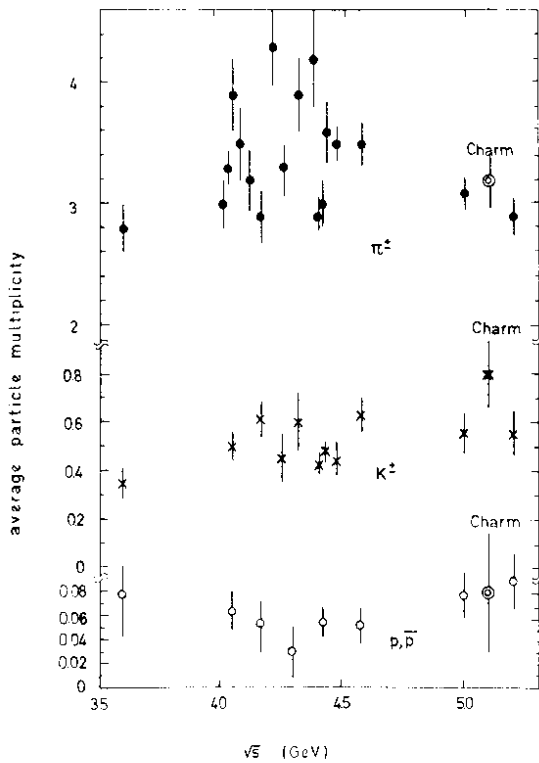line shows the result for pp collisions (Ref. 12).

Fig. 11 Average multiplicity of $\pi^{\pm}$, $K^{\pm}$ and p,$\bar{p}$
per event. The points labelled "charm" give the
multiplcities for charmed events alone. (Ref. 11)

After integrating over the angles one has

$$\frac{d\sigma}{dx} = \frac{4\pi\alpha^2}{s} \ \beta \ x \ \{m\bar{W}_1 + \frac{1}{6} \ \beta^2 x \ \nu\bar{W}_2 \} \tag{5}$$

Since the first term is dominating

$$\frac{d\sigma}{dx} \simeq \frac{4\pi\alpha^2}{s} \ \beta \ x \ m\bar{W}_1 \tag{6}$$

The structure functions $\bar{W}_1$ and $\bar{W}_2$ in general are functions of two variables e.g. s and the scaling variable x which corresponds to the scaling variable $x = 1/\omega$ used in inelastic lepton nucleon scattering. If scale invariance holds $\bar{W}_1$ and $\nu\bar{W}_2$ are functions of x alone and the so called scaling cross section $s/\beta \ d\sigma/dx$ is almost the same for all values of s (see eqs. 5, 6).

Scaling behaviour is e.g. expected from the hypothesis of quark fragmentation: at energies large enough that particle masses can be neglected, the number of hadrons h produced by a quark q with fractional energy x, $D_q^h(x)$, is independent of s. This leads to

$$\frac{d\sigma}{dx}(e^+e^- \to q\bar{q} \to h) = \sigma_{q\bar{q}} \cdot 2D_q^h(x) = \frac{8\pi\alpha^2}{s} \ e_q^2 D_q^h(x) \tag{7}$$

Fig. 13 shows the scaling cross section as measured between 3.6 and 5.2 GeV for $\pi^\pm$, $K^\pm$ and $2\cdot\bar{p}$. Most remarkable is the similarity between the three types of particles. Within a factor of two their cross sections fall on a common curve. Scaling is tested in Fig. 14 where pion data are compared at 3.6 and 5.0 GeV. For $x > 0.3$ scaling is satisfied to within 30 %. Between 3.6 and 5.0 GeV the charmed threshold is crossed leading to a rise of the total cross section by almost a factor of two. From Fig. 14 we see that the additional cross section produces only low x pions.

Fig. 15 compares the scaling cross sections for pions and kaons with inclusive ρ^0 production measured by PLUTO[13] and D production measured by SLAC-LBL[14]. A striking similarity in shape as well as in size is observed for π, K, ρ^0 while D production is a factor of 5 to 10 larger.

At higher energies inclusive cross sections have been measured for the sum of all charged particles. Since the mass of the particle is not known, the scaling variable $x = E/E_{beam}$ is replaced by $x_p = P/E_{beam}$ and the quantity $sd\sigma/dx_p$ is measured instead of $s/\beta \ d\sigma/dx$. (In the following x is used for x_p).

Fig. 16 displays the data from TASSO measured at energies of 13, 17 and 27.4 GeV together with measurements from SLAC-LBL[15] at 3 GeV and DASP[11] at 5 GeV. At $x > 0.2$ the scaling cross sections are found to be the same between 5 and 27.4 GeV within errors (~20-30 %). The rise of the charged multiplicity we saw in Fig. 10 is related to the dramatic increase of the particle yield a low x; for instance at $x = 0.06$ the increase is an order of magnitude going from 5 to 27.4 GeV. The 13 GeV data are somewhat special in that for $x > 0.2$ they are above the values measured for 17 GeV. Since 13 GeV is still close to the $b\bar{b}$ threshold this may indicate copious $B\bar{B}$ production (and decay).
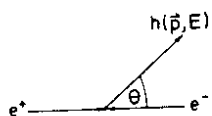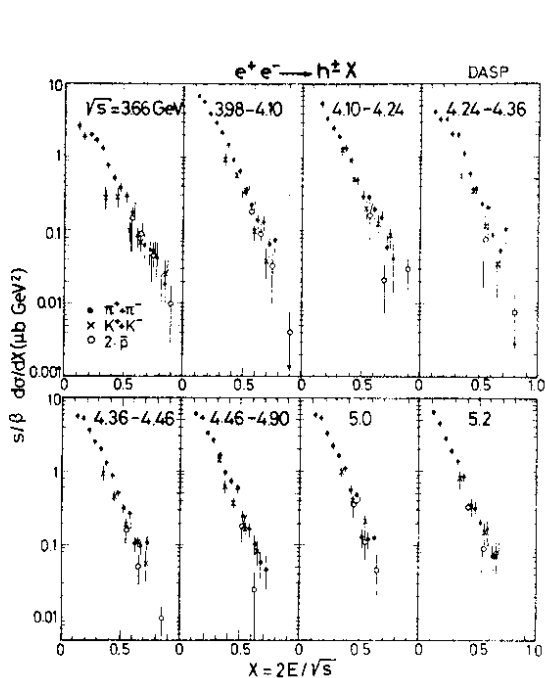
Fig. 12 Diagram for inclusive particle production.

Fig.13 The scaling cross section s/β dσ/dx (x = 2E/√s) as a function of x for the sum of π⁺π⁻, K⁺ and K⁻ and twice the p̄ production for different intervals of the total energy.
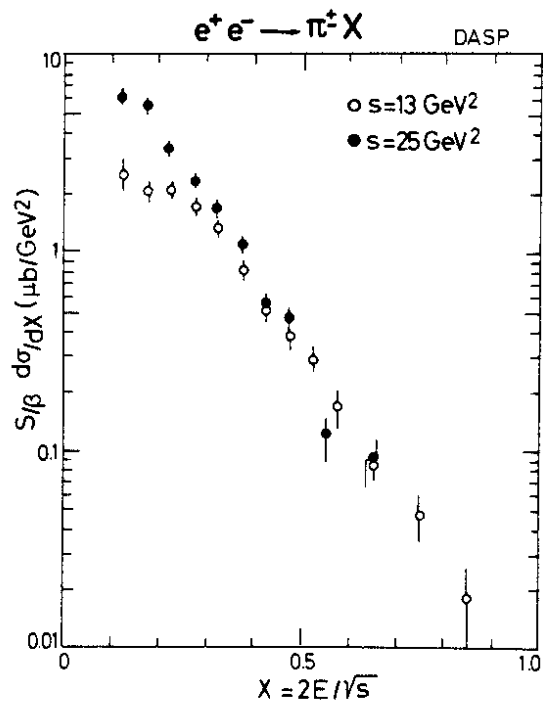
Fig.14 Comparison of the scaling cross sections (s/β) dσ/dx for π± at s = 13 and 27 GeV² (Ref. 11).

Gluon emission will lead to scale breaking effects: the primary momentum is now shared by quark and gluon resulting in a depletion of particles at high x and an excess of particles at low x values. The curves in Fig. 16 indicate the size of the expected scale breaking[16]. It amounts to a 30 % effect at x = 0.6 comparing 5 and 27.4 GeV cross sections. The precision of the data does not allow to test the predicted change.

5. JET FORMATION

As mentioned before the quark model views annihilation into hadrons as a two step process: first, a pair of quarks is produced which then fragment into hadrons (see Fig. 17). If the hadron momenta transverse to the quark direction of flight are limited and the number of produced hadrons grows only logarithmically with energy the emitted hadrons will be more and more collimated around the primary quark directions as the total energy increases and one will observe jets. Let $<n> = a + b \cdot \ln s$ be the average particle multiplicity, $<p_T>$ and $<p_{\parallel}> \approx <p> \approx \frac{\sqrt{s}}{<n>}$ the average transverse and longitudinal hadron momenta then the mean half angle of the jet cone is given by

$$<\lambda> = \frac{<p_T>}{<p_{\parallel}>} \approx \frac{<p_T> \cdot <n>}{\sqrt{s}} = \frac{<p_T> (a + b \cdot \ln s)}{\sqrt{s}} \sim \frac{1}{\sqrt{s}} \tag{8}$$

The jet cone opening angle decreases roughly proportional to $s^{-1/2}$ as the energy increases.

The occurrence of jets in e^+e^- annihilation was first demonstrated in the pioneering work of SLAC-LBL[17]. This work was followed by measurements of PLUTO at energies up to 10 GeV and including neutrals in the jet analysis[18]. The experiments done at PETRA and reported at this conference have extended the jet studies up to 27.4 GeV[8-10,19]. Jet structure is commonly tested in terms of sphericity S and thrust T:

$$S = \frac{3}{2} \frac{\sum p_{\perp i}^2}{\sum p_i^2} \qquad\qquad 0 \leq S \leq 1 \tag{9}$$

and

$$T = \frac{\sum |p_{\parallel i}|}{\sum p_i} \qquad\qquad \frac{1}{2} \leq T \leq 1 \tag{10}$$

where $p_{\parallel i}$, $p_{\perp i}$ are the longitudinal and transverse particle momenta relative to the jet axis which is shosen such that $\sum p_{\perp i}^2$ ($\sum |p_{\parallel i}|$) is minimal (maximal) for sphericity (thrust). Extreme jettiness yields S = 0 and T = 1.

Comparing eq(8) with (9) we see that sphericity has a simple meaning: S measures the square of the jet cone opening angle:

$$S \approx \frac{3}{2} <\lambda^2> ; \tag{11}$$

likewise

$$T \approx \sqrt{1 - <\lambda>^2} \tag{12}$$

In general not all final state particles are detected; e.g. neutrals are usually not registered. As a consequence the reconstruction of the true jet axis is only approximate. The effects of acceptance, detection efficiency and measuring accuracy have to be studied by an elaborate Monte Carlo analysis in order to separate physics effects from systematic biases.
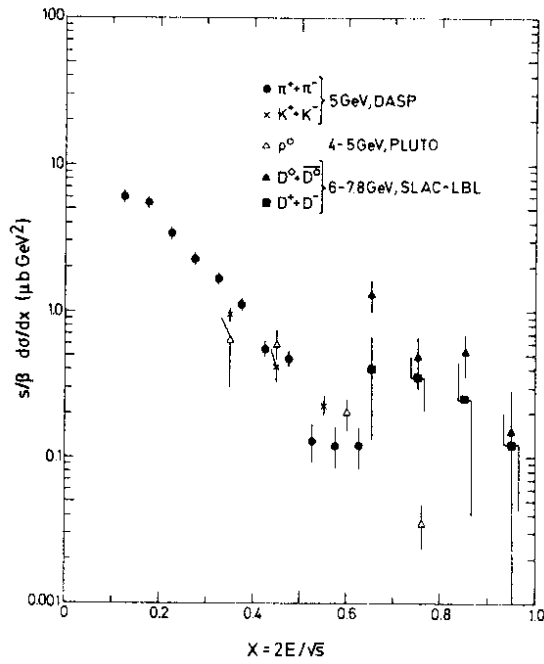
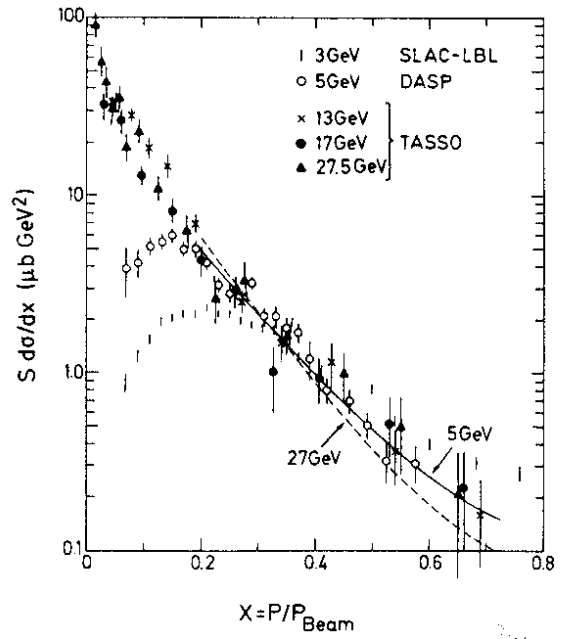Fig.15 The scaling cross section s/β dσ/dx (x = 2E/√s) for π±, K± (Ref. 11) ρ⁰ (Ref. 13), D⁰,D̄⁰ and D± production (Ref. 14).

Fig.16 The scaling cross section s dσ/dx (x = p/p_Beam) for inclusive charged particle production as measured at 3 GeV by SLAC-LBL[15] at 5 GeV by DASP[11] and at 13, 17 and 27.4 GeV by TASSO[10]. The curves show the QCD scale breaking effect predicted for going from 5 to 27.4 GeV[16].

a) Tests for quark jets

Fig. 18 displays the observed mean sphericity as a function of energy measured by SLAC-LBL. This measurement gave the first evidence for jet formation. The sphericity is approximately constant up to 4 GeV and then decreases with increasing energy. The solid and dashed curves show the Monte Carlo results for jet and phase-space like produced events. The theoretical curves have been corrected for acceptance and detection efficiencies. In the jet calculation an average $<p_T>$ of 0.315 GeV/c was assumed. At low energies ($\lesssim 4$ GeV) where $<p_\mu>$ is of the same order as $<p_T>$ both models predict the same average sphericity. Above 4 GeV phase space predicts sphericity to rise contrary to the data while the jet model describes the data well.

Fig. 19 shows a compilation of average sphericity values $<S>$ from PLUTO and TASSO. One finds $<S>$ to decrease from 0.4 at the J/ψ to ~0.15 at 27.4 GeV. The trend to ever stronger collimation persists up to the highest energy explored in agreement with the simple quark model. The jet cone opening angle deduced from $<S>$ is ~31^0 at 4 GeV dropping to 18^0 at 27.4 GeV. A straight line fit to the data in Fig. 19 yields

$$<S> = 0.8 \ s^{-1/4}$$

The shrinkage of the jet cone is slower than expected from the naive arguments given above, $<S> \sim s^{-1}$.

A jet analysis in terms of thrust leads to the same conclusions (Fig. 20). The curve shows the prediction of De Rujula et al. [20].

In Fig. 21 T distributions are shown at low and high energies. The trend towards more and more jetlike events is clearly visible.

The analyses described sofar included only charged particles. PLUTO has investigated also neutral particle (photons) distributions[18]. Define $dE/d\lambda$ to be the energy emitted at an angle λ with respect to the jet axis. Fig. 22 shows at 9.4 GeV the neutral and charged energy flow $dE^0/d\lambda$ (data points) and $dE^C/d\lambda$ (histograms) with respect to the thrust axis which had been determined from charged particles alone. The neutral energy is seen to be concentrated near the jet axis in much the same way as charged particles.

The jet axis distribution around the beam direction provides another test of the quark model. Since quarks have spin 1/2 the polar angular distribution is of the form (neglecting mass effects)

$$d\sigma/d\cos\Theta \sim 1 + \cos^2\Theta \qquad (13)$$

For comparison, spin 0 quarks would lead to

$$d\sigma/d\cos\Theta \sim \sin^2\Theta$$

The experimental data have been found to be consistent with a $1 + \cos^2\Theta$ distribution. The cleanest test has been made by SLAC-LBL studying jet production with beams polarized transverse to the storage ring plane[17]. In this case the angular distribution is of the form

$$d\sigma/d\Omega \sim 1 + \alpha\cos^2\Theta + \alpha P_+ P_- \ \sin^2\Theta \ \cos2\varphi \qquad (14)$$

where the azimuthal angle φ of the jet axis is measured with respect to the storage ring plane, $P_+ (P_-)$ is the degree of polarization and $\alpha = 1$ for $q\bar{q}$ production. Fig.23 shows the φ distribution measured with $P_+ P_- = 0.5$. A fit to the φ distribution yielded $\alpha = 0.97 \pm 0.1$ in agreement with the quark model.
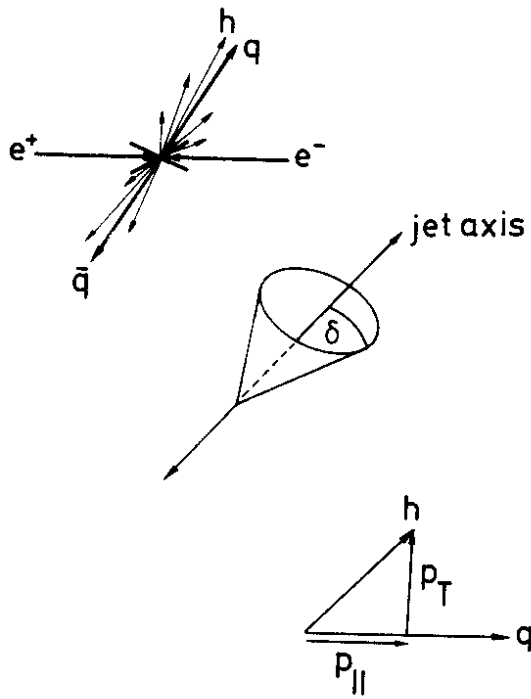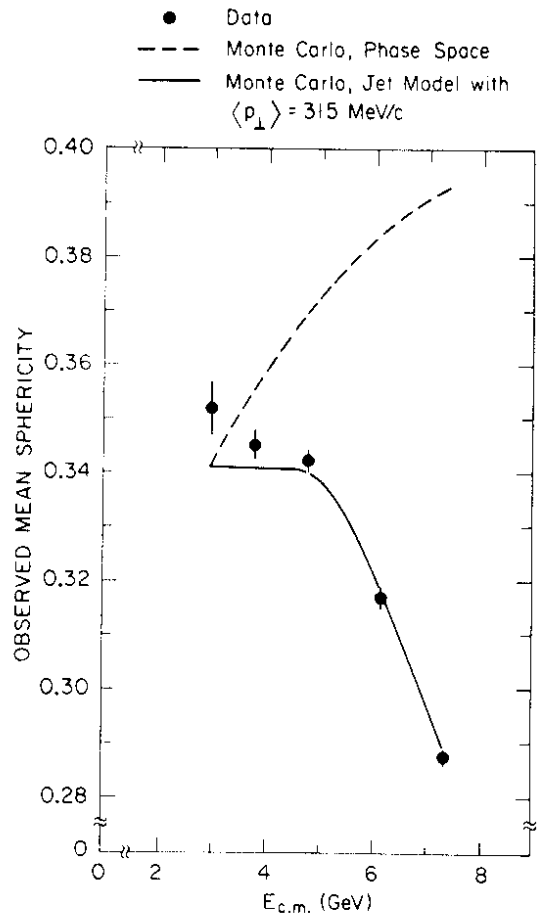
Fig.17 Jet formation

Fig.18 Observed mean sphericity versus total energy. The solid curve is the result of a jet model calculation with <p_T> = 0.315 GeV/c. The dashed curve is the invariant phase space prediction (Ref. 17).
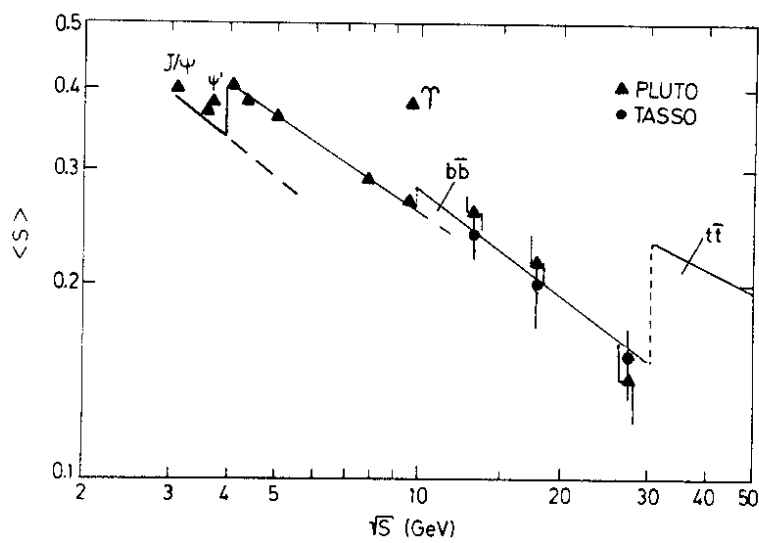

Fig.19 The average sphericity as a function of the total energy as observed by PLUTO (Ref.9, 18) and TASSO (Ref. 10). The curves indicate the expected contributions from u, d, s, c, b and t quark pairs.
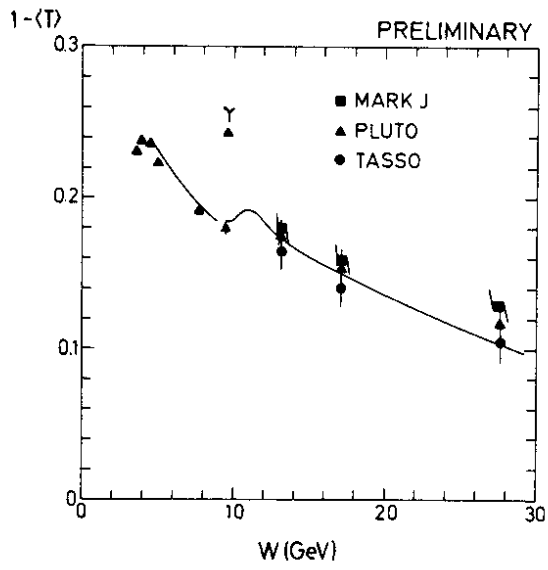
Fig.20 Energy dependence of $1 - <T>$ as measured by MARK J[8], PLUTO[9,18]and TASSO[10]. The curve shows the theoretical prediction[20].
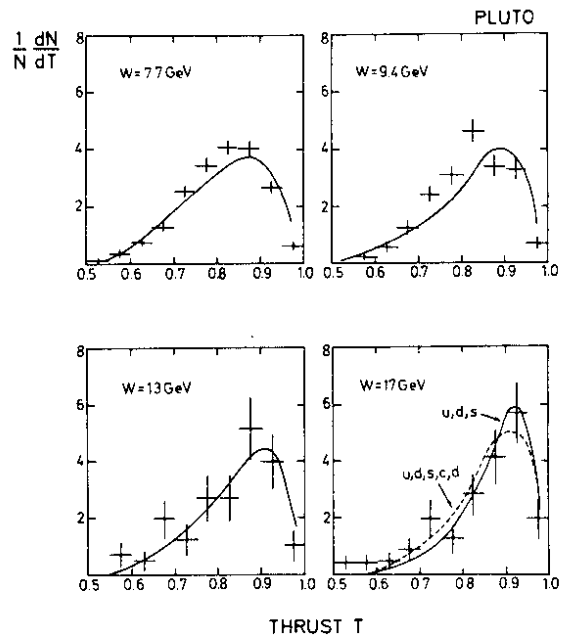
Fig.21 Thrust distributions for different total energies from Ref. 9. The solid and dashed curves show the quark model predictions using Field and Feynman fragmentation functions[21].
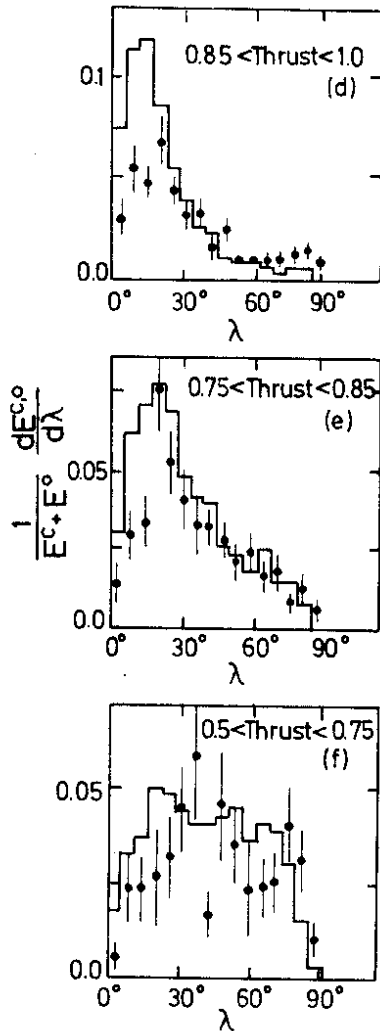
Fig.22 The angular distributions
$1/(E^C + E^0) \cdot dE^0/d\lambda$ of neutral energy (data points) and charged energy
$1/(E^C + E^0) \, dE^C/d\lambda$ (histograms) with respect to the thrust axis at 9.4 GeV for different T intervals. PLUTO (Ref.18).

Fig.23 Azimuthal distribution of the reconstructed jet axis; zero degree is in the ring plane = plane of polarization.
(a) for a total energy of 6.2 GeV where the beam polarization is zero;
(b) for a total energy of 7.4 GeV where the product of the e^+ and e^- beam polarization is $p^2 = 0.5$. SLAC-LBL (Ref.17).

b) Structures in the energy dependence of sphericity

The energy dependence of <S> shown in Fig. 19 exhibits interesting structures. It is large at the J/ψ, ψ' and T with values close to those p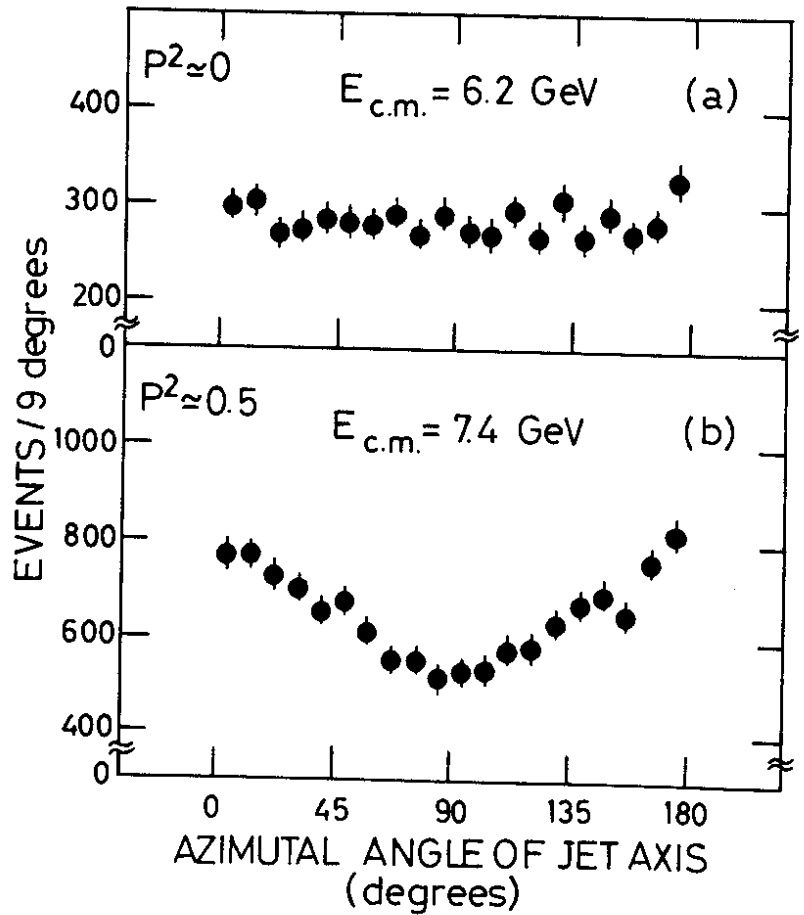redicted by pure phase space (<S> $\simeq$ 0.4 - 0.5) and it shows a rise at 4 GeV above the charm threshold. This rise can be understood as follows. Close to threshold the charm quarks are slow and the final state particles are emitted phase space like. Defining $<S_{ps}>$ and $<S_{2jet}>$ as the average sphericities for phase space and u,d,s produced events respectively, and R_c, $R_{u,d,s}$ the contributions from $c\bar{c}$ and $u\bar{u}$, $d\bar{d}$, $s\bar{s}$ production, the average sphericity just above charm threshold can be computed:

$$<S> = \frac{<S_{ps}> R_c + <S_{2jet}> R_{u,d,s}}{R_c + R_{u,d,s}} \tag{15}$$

One finds e.g. that at 4.5 GeV <S> increases due to the charm contribution by 0.06 from 0.32 to 0.38 in agreement with the data.

As the energy increases the velocity β of the charm quarks grows and the $c\bar{c}$ final states start to become jet like too. One may guess that for $\beta \simeq 0.7$ the increase of <S> due to the $c\bar{c}$ contribution is only half of its value near the threshold. This "half width" point for the $c\bar{c}$ contribution is reached around 5 GeV.

Applying the same receipe to the $b\bar{b}$ contribution <S> is found to increase by ≈ 0.02 at 10 GeV. The increase is small due to the (expected) small $b\bar{b}$ contribution ($R_{b\bar{b}} = 0.3 - 0.6$). The half width point is near 13 GeV.

c) Particle emission with respect to the jet axis

The production of hadrons with respect to the jet axis has been extensively studied. If the quark model is correct these analyses permit in a very clean manner a study of quark fragmentation, clean since e.g. smearing effects due to quark fermi motion in the target are absent. The data have been analysed in terms of the longitudinal and transverse momenta, $p_{||}$ and p_T, the rapidity $y = 1/2 \ln \left[(E + p_{||})/(E - p_{||})\right]$ and the fractional longitudinal momentum $x_{||} = p_{||}/E_{beam}$. Fig. 24 shows rapidity distributions for charged particles for energies between 4.8 and 27.4 GeV. To compute y the particles were assumed to be pions. The normalization is such that $1/\sigma \, d\sigma/dy$ gives the normalized yield <u>per jet</u>. The width of the y distributions increases and some sort of plateau is developing as the energy increases. The height of the plateau is not constant but is rising too. The fragmentation region is approximately two units wide which is equal to what is observed in hadron scattering. The fragmentation region is scaling. That can be seen when the data are plotted with respect to $y_{max} - y$ ($y_{max} \approx \frac{1}{2} \ln \frac{s}{m^2}$) as shown in Fig. 25.

Provided that only one kind of quark pair is produced and that the quarks fragment into pions only, theory predicts a plateau width Δy that grows logarithmically with energy,

$$\Delta y \approx y_{max} - 2 \approx \frac{1}{2} \ln s/m^2 - 2$$

a constant plateau height and scaling in the fragmentation region. The experimentally observed rise of the height of the plateau is related to the more rapid growth of the average particle multiplicity above 10 GeV (see Fig. 10).
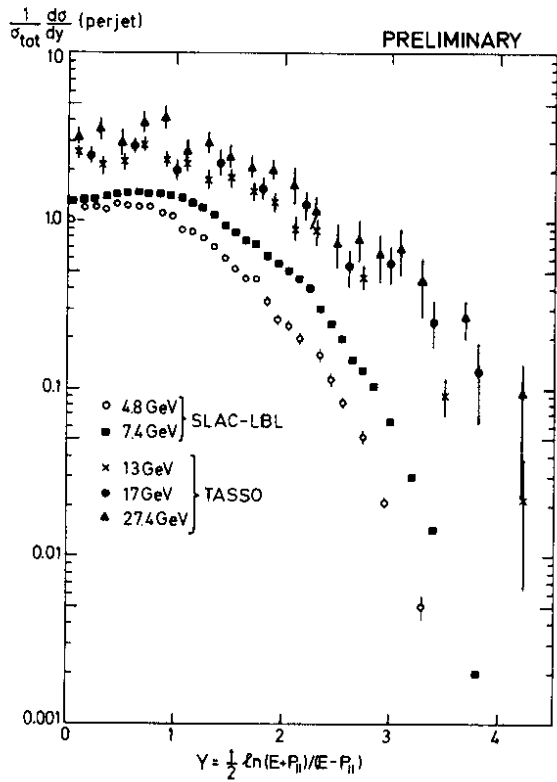
Fig.24 Rapidity distribution for charged
particles assuming m = m$_\pi$: Yield per jet,
normalized to the total cross section.
Measurements by SLAC-LBL (4.8 and 7.4 GeV,
Ref.17) and TASSO (13, 17 and 27.4 GeV,
Ref.10).

Fig.25 Rapidity distributions for charged
particles as a function of y$_{max}$ - y assuming
m = m$_\pi$: Yield per jet normalized to the total
cross section. Measurements by SLAC-LBL (4.8
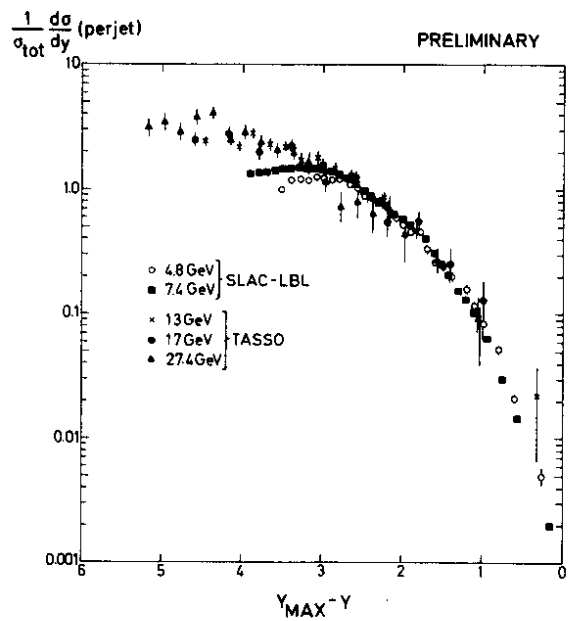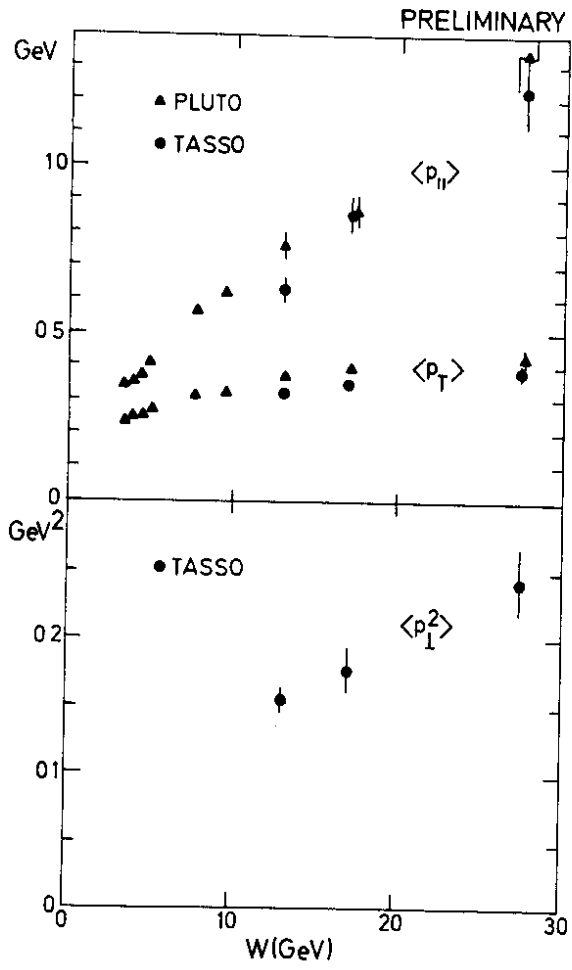and 7.4 GeV, Ref.17) and TASSO (13, 17 and
27.4 GeV, Ref.10).

Fig.26 The energy dependence of $<p_{\shortparallel}>$, $<p_T>$ and $<p_\perp^2>$ relative to the thrust axis for charged particles (from Refs. 9, 10).
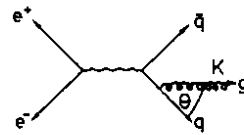

Fig.27 Schematic diagram for gluon emission.

Fig. 26 shows the energy dependence of the average $p_{\parallel}$ and p_T values. The average longitudinal momentum grows almost linearly in accordance with our expectation. The transverse momentum shows a rapid rise below 5 GeV which must be due to the increase in phase space. The data between 6 and 13 GeV are consistent with a constant $<p_T>$. The measurements at the highest energy, 27.4 GeV, show that $<p_T>$ is rising between 17 and 27.4 GeV:

Table 3

Average p_T and p_T^2 values (preliminary)

| W (GeV) | $<p_T>$ in GeV/c | | $<p_T^2>$ in GeV²/c² |
	PLUTO	TASSO	TASSO
13	0.37±0.01	0.329±0.009	0.145±0.010
17		0.363±0.013	0.175±0.014
27.4	0.43±0.02	0.422±0.020	0.276±0.029

As has been discussed by Professor Söding measuring errors can lead to a widening of the $<p_T>$ distribution. However, the increase in $<p_T>$ and in particular in $<p_T^2>$, observed by TASSO cannot be accounted for by instrumental biases or by the larger phase space which allows quarks to fragment more frequently into heavier particles (kaons).

The widening of the p_T distribution is an important prediction of QCD which we will discuss briefly.

6. JET BROADENING BY QCD EFFECTS

Hard gluon emission illustrated by the diagrams b and c of Fig. 7 leads to a broadening of the p_T distribution and of the jet cone as shown by Ellis, Gaillard and Ross [22]. Qualitatively, the broadening of $<p_T>$ can easily be understood. Similar to the emission of photons from an electron the gluon distribution radiated off a quark is approximately given by [23]

$$\frac{d\sigma(q\bar{q}g)}{dk\,d\cos\Theta} = \frac{\alpha_s}{K(1 - \cos\Theta)^2}\, \sigma_{q\bar{q}}$$

$$(16)$$

or

$$\frac{d\sigma(q\bar{q}g)}{dk\,d\Theta} \approx \frac{\alpha_s}{K\sin\Theta}\, \sigma_{q\bar{q}}$$

where K and Θ are the gluon energy and emission angle relative to the quark direction of flight (see Fig. 27). The average transverse momentum of the (hard) gluon jet is

$$<K_T> \approx \frac{\alpha_s \cdot \sigma_{q\bar{q}} \displaystyle\iint \frac{K\sin\Theta}{K\sin\Theta}\, dK\,d\Theta}{\sigma_{q\bar{q}}\,(1 + \frac{\alpha_s}{\pi})}$$

$$\approx \alpha_s \cdot E_{beam} \qquad \text{(up to log terms)} \qquad (17)$$

The remarkable result is that contrary to many other predictions of QCD which lead to logarithmic deviations from the pure quark model, and are therefore difficult to test experimentally, the transverse momentum is predicted to rise linearly with energy. A direct consequence is that the jet cone will not shrink indefinitly but will have an almost constant opening angle, $\delta = <p_T>/<p_{\parallel}>$ since both, longitudinal and transverse momenta, will grow linearly with energy above a certain minimum energy.

Fig. 28 shows the measured sphericity distribution at 27.4 GeV together with the predictions from the pure quark model (including u,d,s,c,b quarks) and the QCD corrections to it[24]. The statistical accuracy is insufficient to prefer one over the other.

The QCD broadening of jets has been extensively studied[20,22,24-27], devising many tests to establish this phenomenon. The distinction between the QCD broadening and e.g. a mere rise of the average p_T for quark fragmentation is possible. The hard gluon emission leads to three jet events or, if you like one fat and one small jet while the latter would produce two fat jets. As shown by Professor Söding in his talk the available data are consistent with QCD. More statistics at high PETRA energies will make the QCD effects clearly discernible from other possible sources.

7. SEARCH FOR THE t QUARK

The observed symmetry between leptons and quarks suggests besides u, d, s, c, b the existence of a sixth quark, t. The charge of the t quark is predicted to be +2/3 if one groups the quarks in weak isospin doublets, viz

$$\begin{pmatrix} u \\ d \end{pmatrix}, \begin{pmatrix} c \\ s \end{pmatrix}, \begin{pmatrix} b \\ t \end{pmatrix}$$

The theoretical predictions for the t mass populate mass values between 10 and 40 GeV[28]. Forgetting about theory one can look at the ψ, J/ψ, Υ mass spacing,

$$m_{J/\psi}/m_\phi \simeq m_\Upsilon/m_{J/\psi}$$

which suggests the $t\bar{t}$ vector ground state to be found at

$$m_{V_t} = m_\Upsilon^2/m_{J/\psi} \simeq 28 \text{ GeV}$$

which is in the reach of PETRA. The peak height of the total cross section at the position of V_t depends on the leptonic decay width Γ_{ee} and on the energy spread of the storage ring beams. The Breit-Wigner without energy spread reads

$$\sigma(e^+e^- \to V_t) = \frac{3\pi}{s} \frac{\Gamma_{ee}\,\Gamma}{(M_0 - W)^2 + \Gamma^2/4} \tag{18}$$

The energy spread of the beams, ΔE, reduces the peak cross section - very roughly - to

$$\sigma_{peak} \simeq \frac{3\pi}{s} \cdot \frac{\Gamma_{ee}}{\Delta W} \tag{19}$$

where $\Delta W = \sqrt{2} \cdot \Delta E$. For PETRA

$$\Delta E/E = 6.5 \cdot 10^{-5} E, \qquad E \text{ in GeV} \tag{20}$$

For a mass of 28 GeV (E = 14 GeV) the energy spread is ΔE = 13 MeV. The leptonic width Γ_{ee} depends on the shape of the $t\bar{t}$ potential. Various models studied[29] suggest that Γ_{ee} is approximately the same as for the J/ψ, Γ_{ee} = 5 keV. This yields

$$\sigma_{peak}(28 \text{ GeV}) \simeq 1.3 \text{ nb}$$

or
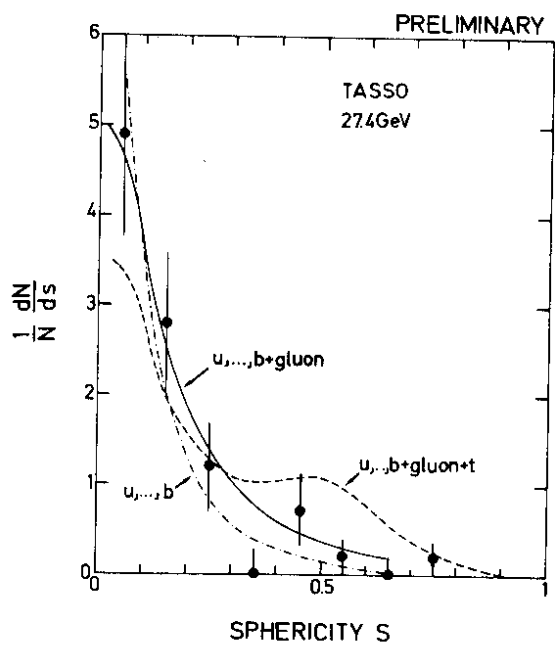
$$R_{peak}(28 \text{ GeV}) \simeq 11.$$

Fig.28 The sphericity distribution at
27.4 GeV as measured by TASSO (Ref.10).
The curves show predictions[24] of the
quark model with u, d,...b quarks
(dashed-dotted) plus gluon corrections
(solid) plus a t quark contribution
(dashed).

The signal to noise ratio is 11:4 or ~3. This may be compared with the J/ψ seen at SPEAR or DORIS where the signal to noise ratio is roughly 100.

The $c\bar{c}$ system has two bound $^3S_1$ vector states, J/ψ and ψ'; the $b\bar{b}$ system probably has three while the $t\bar{t}$ is expected[29] to have 6 or 7 bound states $1^3S_1,\ldots,6^3S_1$ as sketched in Fig. 29. One may guess that the $t\bar{t}$ continuum is likely to begin two or three pion masses above the $T\bar{T}$ threshold (where T denotes a $t\bar{q}$ meson), i.e. $W_{continuum} \approx M(6^3S_1) + 2\div3\, m_\pi \approx M(V_t) + 2$ GeV.

While it will require a large effort to localize the vectorstates it should be straight forward to detect the $t\bar{t}$ continuum contribution provided the available energy is sufficient. The asymptotic $t\bar{t}$ contribution should be $R_t = 3 \cdot (\frac{2}{3})^2 = \frac{4}{3}$. Near threshold it is likely to be larger. Comparing with the charm contribution near 4 - 4.5 GeV, one may expect $R_t = 2$ or $R \simeq 6$ above $t\bar{t}$ threshold. The R values measured by MARK J, PLUTO and TASSO up to 27.4 GeV (see Fig. 6) do not show this expected rise in R from 4 to 6. They are con-
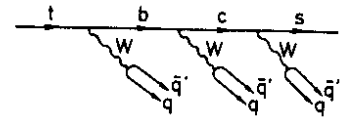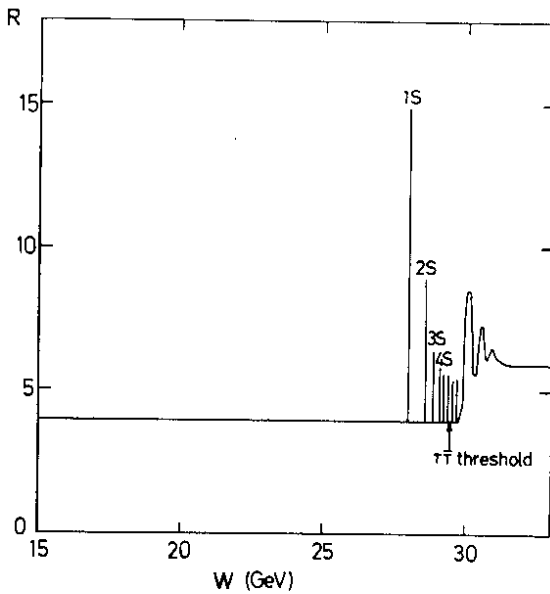

Fig.30 (Hadronic) decay scheme for t quarks.

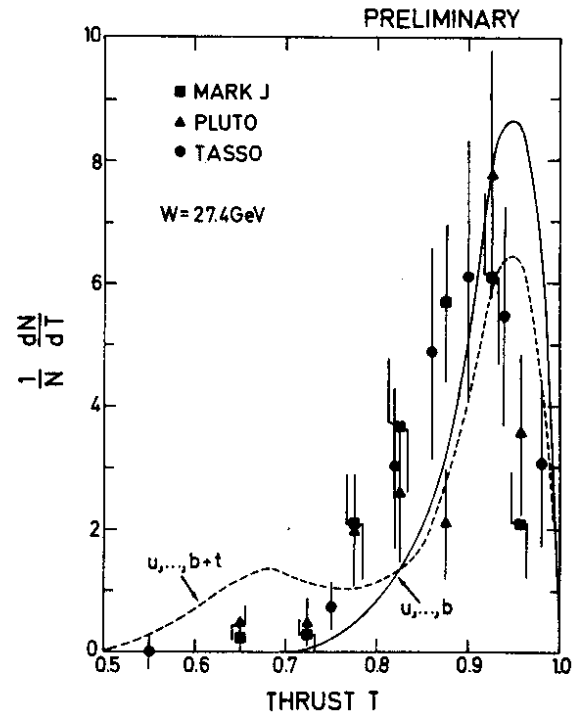Fig.29 The energy dependence of R expected near the $t\bar{t}$ threshold.

Fig.31 Thrust distribution at 27.4 GeV (Refs. 8-10). The curves show the predictions of the quark model for u, d,...b and for a t.

sistent with no rise between 13 and 27.4 GeV. However, the systematic uncertainties quoted are of the order of 10 - 20%.

A quantity more sensitive to the $t\bar{t}$ contribution is the sphericity. Events from $t\bar{t}$ decay can be expected to have high multiplicity and a phase space like configuration near threshold. According to the Kobayashi-Maskawa[30] generalized Cabibbo matrix the favored decay sequence for t quarks is t → b → c → s. As a consequence $T\bar{T}$ hadronic decays have no less than 14 (or more) quarks in the final state (see Fig. 30). The same line of argument used to explain the step in <S> above the charm threshold predicts a large increase of S by ∿ 0.08 from roughly 0.15 below threshold to 0.23 above threshold (see curve in Fig.19). A similar effect would be seen in thrust. The data at 27.4 GeV are consistent with what one expects for u,d,s,c,b contributions alone (see Fig. 19).

Finally, one can investigate the sphericity and thrust distributions at 27.4 GeV. Above the $t\bar{t}$ threshold e.g. the T distribution should be a superposition of a rapidly falling distribution from the first 5 quarks including OCD broadening plus a broad gaussian like distribution centered around T ≃ 0.7 describing $t\bar{t}$ events. In Fig. 31 the thrust distribution as measured by MARK J, PLUTO and TASSO at 27.4 GeV are compiled. The data agree well with the distribution expected from u,...,b quarks; there is no evidence for a $t\bar{t}$ contribution. Table 4 summarized the observed and expected number of low thrust events.

Table 4

Observed number of events with thrust T < 0.75 at 27.4 GeV and expected number of events above the $t\bar{t}$ threshold

	$N_{observed}$	$N_{expected}$
MARK J	1	15
PLUTO	3	11
TASSO	2	9

The absence of a $t\bar{t}$ signal can mean either one of two things : the $t\bar{t}$ threshold is above 27.4 GeV or it is below 27.4 GeV but the $t\bar{t}$ contribution is small because 27.4 is in a valley between two $t\bar{t}$ resonances.[+]

8. TWO PHOTON PROCESSES

So far we have been discussion hadron production through annihilation of electron and positron. As first pointed out by Low[31] there is another class of ee processes where the (virtual) photon clouds of the two beams interact with each other and produce hadrons

---

[+] Note added in proof : Data taken at 27.72 GeV did not show any evidence for $t\bar{t}$ events either which renders the valley hypothesis unlikely.

by $\gamma\gamma$ scattering (see Fig. 32). The cross section is of the fourth order in α but logarithmically rising with energy $\sigma(ee \rightarrow eeX) \sim \alpha^4 \ell n^2 \frac{E}{m_e}$; the logarithms result from integrating the photon spectra. Because of its energy dependence the two photon cross section overtakes the annihilation cross section ($\sigma \sim \alpha^2/E^2$) at some point and two photon scattering becomes the dominant source of hadrons at high energies.

Owing to the bremsstrahlung type energy spectrum of the two photons the total c.m. energy M of the hadron system produced by $\gamma\gamma$ scattering is rapidly falling with M, viz.[32]:

$$\frac{d\sigma(ee \rightarrow eeM)}{dM^2} \approx \frac{\alpha^2}{\pi^2} \left(\ell n \frac{4E^2}{m_e^2} \right) \left(\ell n \frac{4E^2}{M^2} \right) \frac{\sigma(\gamma\gamma \rightarrow M)}{M^2} \tag{21}$$

This permits to separate the two types of processes experimentally even at high energies (see Fig. 3).

The PLUTO group[9] has made a first attempt to measure the cross section for $\gamma\gamma$ scattering into hadrons. One of the scattered electrons has been detected (tagged) in a forward hodoscope while the hadrons produced have been observed in the central detector. The event selection required
1. energy of the tagged electron more than 3 GeV,
2. three or more tracks in the central detector, two of which have to have a transverse momentum relative to the beam pipe of more than 0.3 GeV/c.

The scattering angle of the tagged electron had to lie between 23 and 70 mrad which lead to average Q^2 values of one of the virtual photons of 0.09, 0.11 and 0.3 GeV^2 at total energies of 13, 17 and 27.4 GeV, respectively. In evaluating $\sigma_{\gamma\gamma}$ the Weizsäcker-Williams approximation was applied. This can lead to deviations from the exact result as large as factors of 1.5-2 as shown recently by Kessler and coworkers[33].

Fig. 33 shows $\sigma_{\gamma\gamma}$ as a function of the visible hadron energy. The 13 and 17 GeV data for which $<Q^2> \approx 0.1$ GeV^2 the $\gamma\gamma$ cross section can be described by $\sigma_{\gamma\gamma} \approx (0.3 + 0.9/M_{vis})$ μb, M_{vis} in GeV. The 27.4 GeV data with $<Q^2> = 0.4$ GeV^2 are consistently lower above $M_{vis} = 2$ GeV. Simple vector dominance, replacing the two photons by vector mesons, predicts for $M \gtrsim 2$ GeV

$$\sigma_{\gamma\gamma}^{VDM} \approx \frac{2}{3} \sigma_{\pi N} \left(\frac{\sigma_{\gamma p}}{\sigma_{\pi N}} \right)^2 \approx 0.4 \text{ μb}$$

in qualitative agreement with the data. The factor of 2/3 accounts for the fact that the nucleon is made of three quarks and vector mesons of two. To the VDM result the excitation of resonances specific to the $\gamma\gamma$ channel[34] and possibly quark box diagrams[35] have to be added.

The fact that the $\gamma\gamma$ cross sections deduced from the 27.4 GeV data are lower is expected since at least one of the virtual photons is further off the mass shell. The results on virtual photon nucleon scattering suggest for one photon being off the mass shell

$$\sigma_{\gamma\gamma}(Q^2) \approx \frac{1}{1 + Q^2/0.6 \text{ GeV}^2} \sigma_{\gamma\gamma}(0)$$

in rough accord with Fig. 33.
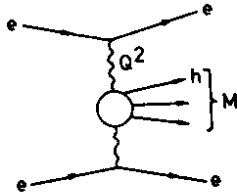
Fig.32 Diagram for γγ scattering.

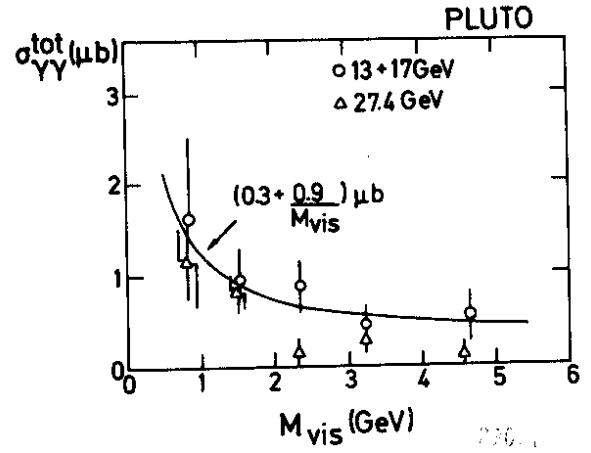Fig.33 The γγ cross section as measured by PLUTO at $\langle Q^2 \rangle$ = 0.1 GeV^2 (13 and 17 GeV data) and 0.4 GeV^2 (27.4 GeV data). (Ref. 9).
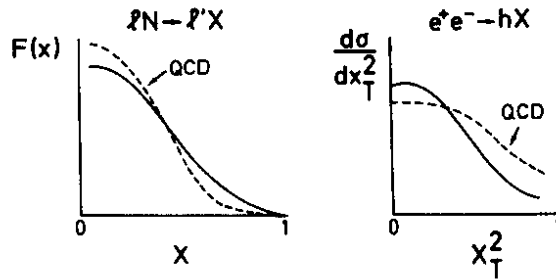

Fig.34 Illustration of QCD effects in lepton nucleon scattering and e^+e^- annihilations.

CONCLUSIONS

1. Hadron production at high energies is dominantly jet-like. The jet cone is shrinking $\sim W^{-1/2}$ as the energy increases.

2. The shape and magnitude of the total cross section, the observed scaling behaviour of the inclusive cross sections, the occurance of jets and their gross features are in astonishing agreement with the quark hypothesis.

3. First evidence for corrections to this hypothesis have been presented to this conference. The momentum distribution of hadrons transverse to the jet axis is broadening at very high energies. The data indicate that only one of the two jets is broadening and that the broadening occurs in a plane. This makes it unlikely that the broadening can be understood as a general widening of the (nonperturbative) P_T distribution with energy. The details of the effects are consistent with QCD where one of the quarks radiates off a hard gluon.

   Deep inelastic lepton nucleon scattering and e^+e^- annihilation complement each other in this respect. The scale breaking observed in the first one is caused by forward emission ($\Theta = 0$) of the gluon, the latter by the transverse momentum component X_T ($\Theta \neq 0$) carried away by the gluon (see Fig. 34).

4. In the energy range up to 27.4 GeV no evidence has been found for the existence of a sixth quark.

5. A first attempt has been made to measure the total $\gamma\gamma$ - cross section. This marks the beginning of a new field : hadron production by the scattering of photons on photons.

REFERENCES

1) A. Quenzer, thesis, Orsay report LAL 1294 (1977);
   A. Cordier et al., Phys. Lett. 81B (1979) 389;
   A.V. Sidorov, rapporteur talk, 1976 Tbilisi Conference, N46

2) G.P. Murtas, 1978 Tokyo Conference, B2;
   R. Baldini, invited speaker at this conference

3) J. Perez-y-Jorba, 1978 Tokyo Conference

4) R.F. Schwitters, rapporteur talk, 1976 Tbilisi Conference, B34

5) Bizot, invited speaker at this conference
   J. Augustin, rapporteur talk to this conference

6) PLUTO collaboration, J. Burmester et al., Phys. Lett. 66B (1977) 395

7) DASP collaboration, R. Brandelik et al., Phys. Lett. 76B (1978) 361

8) MARK J collaboration, D. Barber et al., Phys. Rev. Lett. 42 (1979) 1113

9) PLUTO collaboration, Ch. Berger et al., Phys. Lett. 81B (1979) 410
   and V. Blobel, invited speaker at this conference

10) TASSO collaboration, R. Brandelik et al., Phys. Lett. 83B (1979) 261

11) DASP collaboration, R.Brandelik et al., Nucl. Phys. B148 (1979) 189

12) E. Albini, P. Capiluppi, G. Giacomelli and A.M. Rossi, Nuovo Cimento 32A (1976) lol

13) PLUTO collaboration, G. Knies, rapporteur talk, 1977 Hamburg Conference, p.93

14) P.A. Rapidis et al., SLAC-PUB 2184 (1979)

15) R.F. Schwitters, rapporteur talk, 1975 Stanford Conference, p.5

16) R. Baier, J. Engels and B. Peterson, University of Bielefeld report BI-TP 79/1o (1979)
    adn B. Peterson, private communication;
    W.R. Frazer and J.F. Gunion, University of California report UCD-78-5 (1978)
    and J.F. Gunion, private communication

17) R.F. Schwitters, rapporteur talk, 1975 Stanford Conference, p.5;
    R.F. Schwitters et al., Phys. Rev. Lett. 35 (1975) 1320;
    G.G. Hanson et al., Phys. Rev. Lett. 35 (1975) 1609;
    G.G. Hanson, results presented at the 13th Rencontre de Moriond (1978), Vol. II,
    ed. by J. Tran Thank Van

18) PLUTO collaboration, Ch. Berger et al., Phys. Lett. B78 (1978) 176

19) P. Söding, rapporteur talk at this conference

20) A. de Rujula, J. Ellis, E.G. Florates and M.K. Gaillard, Nucl. Phys. B138 (1978) 387;
    Compared to the original version the nonperturbative part was readjusted;
    J. Ellis, private communication.

21) R.D.Field and R.P. Feynman, Nucl. Phys. B136 (1978)1;
    The production and fragementation of c and b quarks has been incorporated by T. Meyer.

22) J. Ellis, M.K. Gaillard and G. Ross, Nucl. Phys. B111 (1976) 253

23) see e.g. H. Fritzsch, Schladming Lectures 1978, Acta Physica Austriaca Suppl. XIX, p.249

24) P. Hoyer, P. Osland, H.G. Sander, T.F. Walsh, and P.M. Zerwas, DESY report DESY 79/21 (1979);
    and H.G. Sander, private communication.

25) G. Sterman and S. Weinberg, Phys. Rev. Lett. 39 (1977) 1436

26) T. De Grand, Y.J. Ng and S.H. Tye, Phys. Rev. D16 (1977) 3251
    G. Kramer and G. Schierholz, DESY report, DESY 78/62 (1978);
    G. Kramer, G. Schierholz and J. Willrodt, Phys. Lett. 79B (1978) 249

27) G. Fahri, Phys. Rev. Lett. 39 (1977) 1587;
    S. Brandt et al., Phys. Lett. 12 (1964) 57;
    G.C. Fox and S. Wolfram, Nucl. Phys. B149 (1979) 413;
    S.Y. Pi, R.L. Jaffe and F. Low, Phys. Rev. Lett. 41 (1978) 142

28) see e.g. C.J. Aubrecht II and D.M. Scott, COO-1545-247;
    G. Preparata, CERN TH 2599 (1978);
    M.A. Combrugghe, Phys. Lett. 80 B (1979) 365;
    H. Georgi and D.V. Nanopulos, HUTH-78/A039 (1978);
    H. Harari, H. Haut and J. Weyers, Phys. Lett. 78B (1978) 459;
    S. Pakvasa and H. Sugawara, Phys. Lett. 82B (1979) 1o5;
    J.D. Bjorken SLAC-PUB 2195 (1978)
    T.F. Walsh, DESY Report DESY 78/68 (1978)

29) C. Quigg and J.C. Rosner, Phys. Lett. 72B (1978) 462;
    G. Bhanot and S. Rudaz, Phys. Lett. 78B (1978) 119;
    H. Krasemann and S. Ono, DESY-Report DESY 79/09 (1979)

30) M. Kobayashi and K. Maskawa, Pro. Theor. Phys. 49 (1973) 652

31) F.E. Low, Phys. Rev. 120 (1960) 582;
    F. Calogero and C. Zemach, Phys. Rev. 120 (1960) 1860;
    A. Jaccarini, N. Arteaga-Romero, J. Parisi and P. Kessler,
    Compt. Rend. 269 B (1969) 153, 1129; Nuovo Cimento 4 (1970) 933;
    S. Brodsky, T.Kinoshita and Terazawa, Phys. Rev. Lett. 25 (1970) 972;
    H. Terazawa, Rev. Mod. Phys. 45 (1973) 615

32) S. Brodsky, SLAC-PUB 2240 (1978)

33) C. Carimalo, P. Kessler and J. Parisi, Collège de France report L.P.C. 79-06 (1979)

34) see e.g. B. Schrempp-Otto, F. Schrempp, and T.F. Walsh, Phys. Lett. 36B (1971) 463;
    G. Schierholz and K. Sundermeyer, DESY Report 71/49 (1971)

35) M. Greco and Y. Srivastava, University of Rome preprint (1978)